Specific behavior of β-zeolites upon the modification of the surface acidity by Cs and Li exchange†

Sergio Ramírez,[a] José M. Domínguez,[b] Margarita Viniegra[a] and Louis C. de Ménorval[c]

[a] *Departamento Química, Universidad Autónoma Metropolitana, Av. Michoacán y Purísima S/N, México, D. F., México*
[b] *Instituto Mexicano del Petróleo, STI, Programa de Simulación Molecular, Eje Central L. Cárdenas 152, 07730 México D. F., México*
[c] *Laboratoire de Matériaux Catalytiques et Catalyse en Chimie Organique (CNRS UMR 5618), ENSCM, 8 rue de l'Ecole Normale, 34296 Montpellier cédex 05, France*

Received (in Montpellier, France) 14th October 1999, Accepted 2nd November 1999

A study on the modification of the surface acidity of beta zeolite exchanged with Cs and Li was carried out by means of X-ray diffraction, nitrogen adsorption (BET), ^{27}Al-MAS-NMR, (^{133}Cs, ^{6}Li)-MAS-NMR, surface paramagnetic shift (SUPAS) with adsorbed O_2, FTIR of adsorbed pyridine and NH_3-TPD. An inverse correlation between the amount of cations exchanged and the number of acid sites was verified, as well as a gradual decrease of the micropore surface area, *i.e.* a 38% negative variation for the fully exchanged solids ZβCs2 and ZβLi3. The ^{133}Cs and ^{6}Li (SUPAS)-MAS-NMR technique suggested that Cs cations were located in accessible sites, while Li cations were inaccessible and possibly located in cavities within the channels network. The crystallinity of the original beta zeolite was modified slightly after the ion exchange and no trace of amorphous material was detected by XRD and ^{27}Al-MAS-NMR techniques. By means of NH_3-TPD it was found that at similar cation molar concentrations the number of acid sites was about 4 times higher for Li-exchanged zeolites, therefore Cs showed a stronger neutralization power of the acid sites.

Zeolites have many applications in adsorptive and catalytic processes for the oil refining industry.[1] Owing to their acidic properties these solids are a primary choice for substituting chlorinated alumina in metal supported catalysts for paraffin isomerization and aromatization reactions.[2] Some zeolites like HY and ZSM series are widely used in the industry for fluid catalytic cracking (FCC) and lubricant oil hydrodewaxing processes, respectively.[3,4] Nevertheless, for some applications the high surface acidity of zeolites may produce some undesired reactions like cracking,[5] and for this reason great efforts have been made to control their surface acidity, for example by modifying the Si : Al ratio through dealumination[6] or by ion exchange.[7] In many hydrocarbon reactions these procedures do control the formation and rearrangement of carbonium ions.

The synthesis and textural properties of beta zeolite have been reported extensively[8–12] and techniques like HREM,[13] NH_3-TPD,[14,15] ^{27}Al-MAS-NMR and FTIR[16–19] have been applied to characterize the properties of the solids, as for example, the chemical changes occurring on the zeolite surface upon incorporation of alkaline cations and their influence on the catalytic properties.[7,20] The Pt supported on exchanged zeolites exhibited a catalytic selectivity for the *n*-hexane aromatization reaction higher than on the non-exchanged supports, as is the case for Pt/KL zeolite.[7] Alternatively, supported metal catalysts like Pt/β-zeolite showed an enhanced sulfur resistance, and better stability with respect to the KL supported catalysts.[7]

The purpose of the present work was twofold: firstly, to study the influence of alkaline monovalent cations like Cs and Li on the acidic properties of the beta zeolite, and secondly, to study the control of the surface acidity properties for preparing bifunctional Pt/β-zeolite reforming catalysts. To this end, several techniques were used to characterize the textural, structural and acidic properties of the ZβH (acidic) and ZβM (M = Cs, Li) solids, including N_2 adsorption (BET), XRD, ^{27}Al-MAS-NMR, NH_3-TPD and FTIR of adsorbed pyridine.

Also, a new NMR method that takes advantage of the paramagnetic effect of adsorbed O_2 molecules on specific cations in dehydrated zeolites was used. This method, (^{6}Li, ^{23}Na) (SUPAS)-MAS-NMR has proven to be useful in determining the location of the exchanged cations within the zeolite framework.[21,22]

Experimental

The starting material was a commercial zeolite from PQ Corporation (Valfor CP811BL-75). The main chemical and physical properties of this zeolite are summarized in Table 1, where one observes that the Na_2O content is limited to 26 ppm according to the chemical analysis, but the datasheet from the

Table 1 Physicochemical properties of ZβH zeolite

	Reported[a]	This work[b]
Chemical composition		
Al_2O_3/wt%	2.5	2.53
SiO_2/wt%	96.8	97.39
Na_2O/wt%	0.01	0.0026
Si : Al/molar	32.85	32.66
X-Ray diffraction		
Crystalline phase	β-Zeolite	β-Zeolite
Crystallinity/%	85	90
Textural properties		
Surface area/m^2 g^{-1}	725	742

[a] Datasheet from PQ Valor Corp. [b] Chemical composition by AAS.

† *Non-SI unit employed*: 1 Torr ≈ 133 Pa.

supplier reports 100 ppm of Na_2O. The main difference between these values is most probably related to the statistical sampling procedures. The Si : Al ratio was determined by atomic absorption spectrometry (AAS).

The alkaline ion exchange was performed using aqueous solutions of LiOH (Rosemount), CsOH and CH_3COOLi (monohydrated form, Aldrich). The pH values of the starting alkaline solutions were 13.5, 13.9 and 8.1, respectively. The volume : solid ratio in the mixture was 1.7. The initial cationic solutions were 2.15 wt% for Cs and 0.11 wt% for Li; these solutions were diluted in order to achieve the desired concentration of the cation in each solid. The solutions were added dropwise to the zeolite, which had been suspended previously in deionized water and the pH was in the range of 6.5–7.0 during the ion exchange process. After stirring for 12 h the exchanged materials were filtered and washed thoroughly with deionized water, and dried in two steps, first at 313 K and then at 383 K for 1 h, followed by calcination in air at 823 K for 3 h under shallow-bed conditions. Afterwards, the samples were stored under N_2. Using this procedure, several protonic beta zeolite samples were partially or fully exchanged with alkaline ions (Cs, Li). The level of exchange was calculated relative to the aluminum content determined by AAS. Other exchanged samples (ZβCs3, ZβCs4, ZβLi4, ZβLi5 and ZβLi6) were synthesized in the same manner in order to have a more complete series to compare the total number of acid sites as a function of cation concentration.

The micropore surface area of the samples was determined by means of the BET method, using an ASAP 2000 sorptometer. The X-ray diffraction patterns were recorded using a Siemens D-5000 instrument fitted with a monochromator for CuKα radiation.

The ^{27}Al-MAS-NMR spectra were recorded at 78.21 MHz using a Bruker ASX-300 spectrometer; the samples were introduced in the rotor after being stored under ambient conditions, the spinning speed was 12 KHz and an $Al(NO_3)_3$ solution was used as external reference.

The ^{133}Cs- and ^{6}Li-MAS-NMR spectra were recorded using a Bruker ASX-400 MHz spectrometer. For ^{133}Cs experiments at 52.49 MHz, the pulse had a width of 5 μs, the spinning speed was 3 KHz with a pulse delay of 2 s; 15 000 averaged scans were acquired, and a 1 M CsCl solution was used as the external reference. For ^{6}Li at 58.88 MHz, the pulse width was 10 μs, the spinning speed was 3 KHz, with a pulse delay of 10 s and 6000 averaged scans; a 1 M LiCl solution was taken as the external reference. The samples were treated at 673 K under vacuum and the measurements were done with different O_2 pressures in a 5 mm NMR tube, which was sealed for the NMR measurements. A specially designed homemade NMR probehead for spinning the sealed tubes up to 4 kHz[23] was used.

The number of acid sites was determined by NH_3-TPD using a thermal conductivity detector fitted to a GC. The samples were pretreated under helium flow at 2 L h^{-1} with the temperature being varied from room temperature up to 923 K over 1.5 h. Pulses of anhydrous ammonia were injected, at 473 K, until saturation. Then, a He flow was admitted and the temperature was decreased down to 413 K. Ammonia desorption was followed over the interval between 413 K to 873 K with a heating rate of 10 K min^{-1} and a helium flow of 2 L h^{-1}. The amount of NH_3 desorbed per gram of catalyst was determined from the area under the curve.

The nature of the surface acid sites, Brönsted or Lewis, was determined by FTIR spectroscopy of adsorbed pyridine, using a Nicolet 170SX instrument. Self-supported wafers (13 mm diameter) were introduced into a Pyrex glass cell with CaF_2 windows and were pretreated under vacuum (10^{-6} Torr) at 673 K, for 1 h. The adsorption of 20 Torr of pyridine (Merck, spectrophotometric grade) was performed at room temperature over 30 min; then, the gas phase pyridine was removed by vacuum at the same temperature for 30 min. The spectra were recorded at various temperatures, from room temperature up to 773 K. For the calculations the integrated absorbance of the bands at 1545 cm^{-1} (Brönsted) and 1450 cm^{-1} (Lewis) were considered, according to the transmission factors reported by Emeis.[24]

For comparison purposes, commercial -alumina from Kali Chemie (GAKC) and an industrial catalyst from Instituto Mexicano del Petróleo (APt-1) were also studied.

Results

Textural properties

Table 1 shows the surface area of the starting material (ZβH from PQ) determined by nitrogen adsorption (BET). The values reported by the supplier and the one determined in this work were 725 and 742 m^2 g^{-1}, respectively. The corresponding micropore volume was 0.19 cm^3 g^{-1}, which is a typical parameter for a microporous beta zeolite.[14]

The samples studied appear in Table 2 and according to the calculated amount of alkaline ions, ZβCs1, ZβLi1 and ZβLi2 samples were partially exchanged, having an exchange ratio lower than one. On the other hand, the fully exchanged zeolites like ZβLi3 had an exchange ratio greater than the stoichiometric one. The ZβCs2 sample was prepared in order to achieve a complete ion exchange by the addition of a stoichiometric amount of Cs cations. The main textural parameters of the samples are also reported in Table 2. The micropore surface area compared to the original ZβH zeolite decreased by 7% after an exchange level of 30% with Cs for the ZβCs1 sample. For a Cs exchange level of 98% (ZβCs2) the corresponding decrease in the micropore surface area reached 38% for the sample. For the ZβLi1, ZβLi2, ZβLi3 samples having exchange levels of 81, 87 and 110%, the decrease in micropore surface area was 6, 31 and 38%, respectively.

Table 2 Exchange level, acid sites and micropore surface area of various zeolites

	Precursor salt	Cation/ wt%	Exchange level	Acid sites/μmol NH_3 g^{-1}	NH_3 : Al/ molar	Micropore surface area/ m^2 g^{-1}
ZβH	—	—	0	472	1.02	464
ZβCs1	Hydroxide	2.02	31	251	0.55	431
ZβCs2	Hydroxide	6.44	98	71	0.15	289
ZβLi1	Acetate	0.28	81	305	0.63	436
ZβLi2	Acetate	0.30	87	261	0.53	319
ZβLi3	Hydroxide	0.33	110	260	0.52	289
γ-Alumina[a]	—	—	—	310	—	—
APt-1[b]	—	—	—	370	—	—

[a] Commercial support from GAKC. [b] Commercial Pt–Re catalyst.

Structural properties

The X-ray diffraction patterns corresponding to ZβH and ZβM (M = Cs, Li) are displayed in Fig. 1. The inspection of these diffractograms confirms that no important structural variations occurred in the original zeolite after the ion exchange, but only a slight broadening of the (302) diffraction peak appearing at 22.1°(2θ) was apparent for the ZβCs2 material. The ^{27}Al-MAS-NMR spectrum of ZβH (in the hydrated form) is shown in Fig. 2. It is composed of two peaks, one of them corresponding to Al_{Td}, with $\delta \approx 56$ and the other to $Al_{Td\text{-}Oh}$, with $\delta \approx 0$, the latter being *ca.* 7% of the total area. These two signals were also observed by Perez–Pariente *et al.* in this type of zeolite.[16] Fig. 2 also shows the ^{27}Al-MAS-NMR spectrum of ZβCs1 (31% exchange level), still having *ca.* 5% of $Al_{Td\text{-}Oh}$, with respect to total area. In contrast to this behavior, ZβLi3 showed only a single peak at $\delta = 56$, *i.e.*, the Al_{Td} peak. The remainder of the samples, ZβLi1, ZβLi2 and ZβCs2 (spectra not shown), had a similar behavior according to their exchange level; those with a higher exchange level presented only one signal (ZβCs2) and those with lower exchange levels (ZβLi1, ZβLi2) presented two signals.

Fig. 3 shows the ^{133}Cs- and ^{6}Li-MAS-NMR spectra of the ZβCs2 and ZβLi2 dehydrated samples under various O_2 pressures, from 0 to 1800 Torr. The ^{133}Cs-MAS-NMR spectrum measured under vacuum at room temperature (panel *A*, spectrum *a*) exhibited only one peak at $\delta = -194$, indicating a single chemical environment for the Cs cations located at the

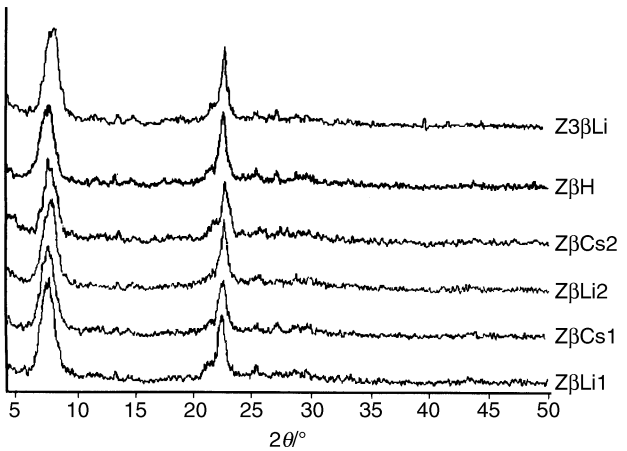

Fig. 1 X-Ray diffraction patterns of ZβH, ZβCs and ZβLi beta zeolite series.

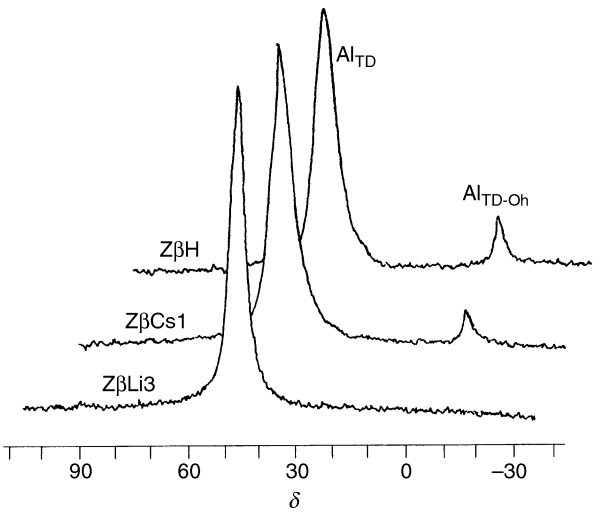

Fig. 2 ^{27}Al-MAS-NMR spectra of ZβH, ZβCs1 and ZβLi3. The spectra have been shifted relative to the *x* axis.

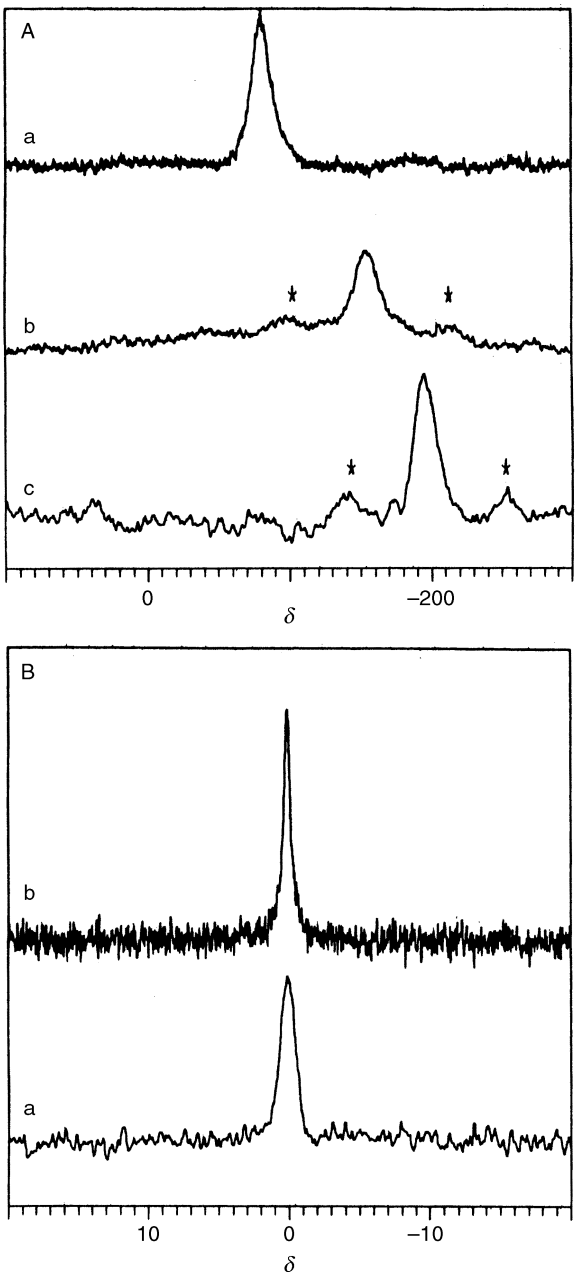

Fig. 3 (A) ^{133}Cs- and (B) ^{6}Li-MAS-NMR spectra of ZβCs and ZβLi zeolites under various oxygen pressures. (A) P_{O_2} (*a*) 0, (*b*) 600, (*c*) 1800 Torr. (B) P_{O_2} (*a*) 0, (*b*) 1800 Torr. The starred peaks are the spinning side bands.

exchange positions of the zeolite. When O_2 is introduced to the sample, the Cs peak shifted to lower field, indicating an effect due to the presence of paramagnetic O_2 molecules near the Cs cations (spectrum *b*). As the O_2 pressure increased to *ca.* 1800 Torr (spectrum *c*), the Cs peak shifted to an even lower value of $\delta = -80$, confirming the paramagnetic shift due to the presence of increasing quantities of physisorbed O_2 in the pores of the beta zeolite.

In the ^{6}Li-MAS-NMR experiments [Fig. 3(*B*)], only one signal was obtained, ($\delta = -0.1$) even at high pressures of O_2 (*ca.* 1800 Torr).

Surface Acidic Properties

The number of acid sites was determined by means of the NH_3-TPD method in the range 413 K $\leqslant T \leqslant$ 773 K and these results are condensed in Table 2. There is a general trend for the amount of NH_3 adsorbed on the Cs- and Li-exchanged series. ZβCs1 and ZβCs2 desorbed 47 and 85% less

ammonia, respectively; ZβLi1, ZβLi2 and ZβLi3 showed a maximum decrease of about 45%. As expected, these results indicate that increasing the cation concentration, either Cs or Li, provokes a diminution of the number of acid sites. The comparison of the number of acid sites for the complete series is shown in Fig. 4, including the additional samples of Cs and Li exchanged zeolites prepared. It is observed that the Cs series presents a greater decrease in the number of acid sites than the Li series (the difference being about 200 μmol NH_3 g^{-1}). It is important to note that the amount of NH_3 desorbed from the Cs series was always lower than from the Li series. Both series show NH_3 desorption, even for high exchange levels. Under the same experimental conditions, the amount of acid sites follows the sequence: ZβH > APt-1 > GAKC > ZβLi(series) > ZβCs(series).

As observed in Table 2, some of the Li exchanged solids had similar values to that of the commercial alumina support. From the number of NH_3 molecules adsorbed per Al atom one observes that ZβH adsorbs one NH_3 molecule per tetrahedral aluminum, while the other solids showed a marked decrease of this ratio, particularly ZβCs2.

Fig. 5 shows NH_3-TPD desorption profiles for ZβH and ZβLi1 samples, where it can be observed that there is an important decrease in the number of acid sites, with a concomitant decrease in the maximum of the desorption temperature and therefore the acid strength. It is also important to note that ammonia desorption starts at temperatures higher than 450 K, as was observed by others.[17]

The nature of the surface acid sites was investigated by means of FTIR spectrometry, using pyridine as a probe molecule from room temperature to 773 K. These spectra (not shown) clearly presented an IR band at 1545 cm^{-1} corresponding to Brönsted sites as well as IR bands in the interval 1445–1455 cm^{-1}, which are commonly assigned to Lewis sites.[17–19] A calculation of the amount of pyridine adsorbed on those sites was performed using the molar extinction coefficients[24] and the results are expressed in micromol of pyridine per gram of zeolitic material, μmol Py g^{-1}. Although this method implies some experimental errors coming from the ε values, valuable information can be obtained on a relative scale, when comparing the results obtained from different samples within a series.[19] The variation with temperature of the amount of pyridine adsorbed on Brönsted and Lewis sites leads to the curves displayed in Fig. 6. There is a clear-cut correlation between the cation concentration (Cs, Li) and the amount of pyridine adsorbed on acid sites, as well as a decrease of the IR peak areas with temperature. ZβH [Fig. 6(A)] had the highest amount of pyridine adsorbed on Brönsted acid sites over the whole temperature range. This amount of adsorbed pyridine diminished for the exchanged zeolites. The ZβCs1 and ZβCs2 samples showed a decrease in the Brönsted site population of about 75 and 100% with respect to ZβH at 473 K. In all of the samples the population of Brönsted sites began to decrease at about 573 K, suggesting that a strong Brönsted acidity is present.

The typical IR bands associated with Lewis sites showed a different behavior with respect to their Brönsted counterparts. For example, the population of the Lewis sites in ZβH decreased with increasing temperature, Fig. 6(B). The trend was more pronounced for ZβCs1 and ZβCs2, which presented no Lewis sites at 573 K. On the other hand, the ZβLi series showed a steady variation of the relative amount of pyridine adsorbed on the Lewis sites. ZβCs2 and ZβLi3, which had no Brönsted acidity, decreased their population of Lewis sites by one-half to one-third with respect to ZβH. The ZβLi1, ZβLi2 and ZβLi3 solids were able to adsorb a higher amount of pyridine on Lewis sites. The shape of the curves in Fig. 6(B) allowed us to conclude that most of these sites are rather weak.

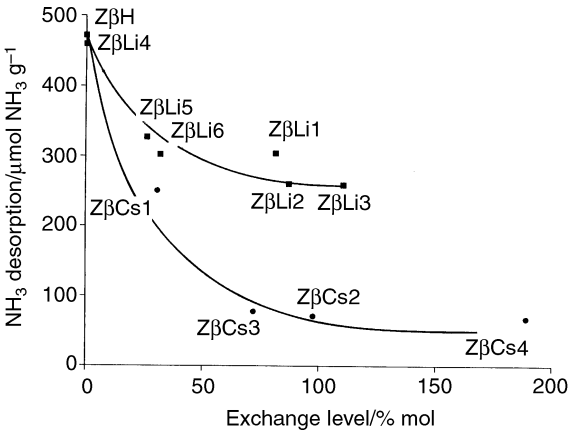

Fig. 4 Number of acid sites, as determined by NH_3-TPD, of exchanged beta zeolites as a function of Cs and Li exchange level.

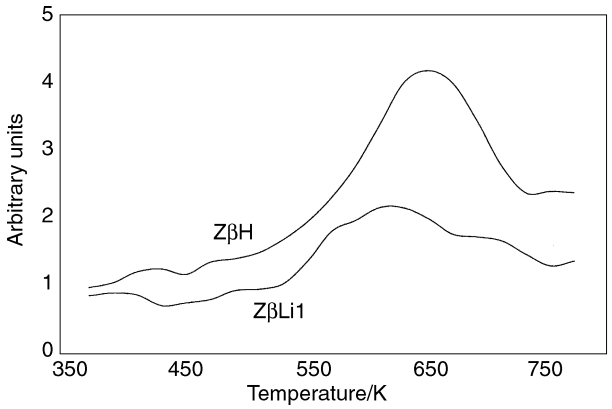

Fig. 5 Ammonia desorption profile from NH_3-TPD of ZβH and ZβLi1.

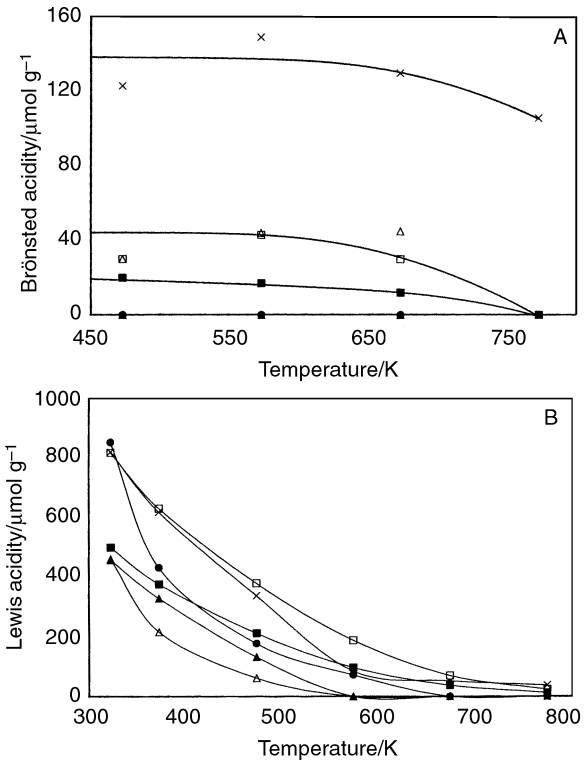

Fig. 6 Brönsted and Lewis acid site distribution determinated by FTIR of adsorbed pyridine *vs.* temperature for acidic and exchanged beta zeolites. (×) ZβH, (△) ZβCs1, (▲) ZβCs2, (□) ZβLi1, (■) ZβLi2, (●) ZβLi3.

In summary, the Cs exchanged zeolites, ZβCs1 and ZβCs2, had weaker acid sites than their Li exchanged counterparts. The strongest sites of ZβH were neutralized more selectively by Cs exchange than by Li exchange, as shown in Fig. 6, where one observes that at a temperature of *ca.* 573 K the amount of pyridine adsorbed on ZβCs1 and ZβCs2 was zero in the Lewis region. At this temperature, in the Li series, both Brönsted and Lewis sites are still present.

Discussion

It was shown that the crystalline structure of beta zeolite was only slightly modified as a consequence of the chemical and thermal treatments that were applied during the ionic exchange. A slight broadening of the (302) diffraction peak at 22.1° (2Θ) was observed, and this may indicate an increase in the crystal size of the zeolite when comparing ZβCs2 and ZβH. This broadening could also be explained by a partial loss of crystallinity, however this is less likely in view of the ^{27}Al-NMR results, *i.e.* the absence of the line at 0 ppm (*vide infra*). Work is in progress in order to clarify this particular point, following in detail the XRD pattern (interplanar distances and crystal size) of the zeolites as a function of the cation concentration.

The cation content of the samples was verified by chemical analysis for distinct precursor salts upon ion exchange, *i.e.*, lithium acetate or lithium hydroxide (Table 2). The precursor salt used did not have any important influence on the final samples.

Strong variations of micropore surface area of our samples as a function of Cs and Li exchange level were observed. There was a micropore surface area reduction equivalent to 38 and 31% (Table 2) for ZβCs2 and ZβLi2, respectively. The exchange level of these samples was near 100%. Thus, the decrease in the surface area calculated by nitrogen adsorbed at 78 K in the samples is probably due to steric effects (blockage of the micropores) rather than to a loss of crystallinity (amorphization) due to the reason stated above.

The ^{27}Al-MAS-NMR representative spectra presented in Fig. 2, for ZβH, ZβCs1 and ZβLi3, show that the first two samples presented a signal at $\delta = 0$ regularly ascribed to octahedral aluminum. The other band, situated at $\delta = 56$, corresponds to Al species having tetrahedral symmetry, Al_{Td}. The fact that ZβLi3 did not show a signal corresponding to octahedral aluminum demonstrates the absence of extra framework aluminum (EFAl) in these samples. The line at $\delta = 0$ corresponds in fact to tetrahedral framework aluminum species bearing H^+ counter ions that can coordinate to water ligands, changing their configuration in a reversible process, as has been stated by several authors.[26,27] For partially exchanged Cs and Li samples, the intensity of the $\delta = 0$ line decreased as the exchange level was increased, indicating that Cs and Li are homogeneously distributed among the Al_{Td} and $Al_{Td\text{-}Oh}$ sites. Therefore, we can conclude that no EFAl species are present, especially at the high cation concentrations in the zeolites studied. If amorphization were occurring octahedral Al should be present, especially at high cation concentrations.

The observed paramagnetic effect in the (SUPAS)-MAS-NMR spectra arises primarily from hyperfine interactions of the unpaired electron spin of the O_2 molecules with the nuclear spins and it depends on the configurations of the observed atoms in the paramagnetic species system.[28–31] These experiments demonstrated that Cs cations are all located in accessible positions on the surface of the channels of the beta zeolite. In this position, Cs cations can experience an interaction with the physisorbed O_2 molecules diffusing in the zeolite channels, leading to a paramagnetic shift of the Cs line. On the other hand, the ^{6}Li (SUPAS)-MAS-NMR with adsorbed O_2 experiments demonstrated that Li cations were not accessible to this gas, since these cations did not present a paramagnetic line shift. This suggests that Li^+ is located in small cavities and not on the surface of the channels of the zeolite.

In regards to the NH_3-TPD and FTIR of pyridine, the results showed that both the concentration and the type of cation exchanged determine the number of acid sites, assuming a one to one stoichiometry, as well as their nature. The Cs series differs from the Li series in that for the former no Lewis acidity is found at temperatures higher than 573 K and therefore, the Lewis acid sites that are present in the Cs exchanged samples are weaker than those of Li exchanged solids or ZβH. Cs also appears to neutralize more effectively the acid sites of the zeolite, the amount of NH_3 desorbed as a function of the exchange level decreases faster for the Cs series than for the Li series. Moreover, the difference in the number of acid sites measured by NH_3-TPD is close to 200 μmol g^{-1} for these two series (Fig. 4). This can be a result of the size of the cation and/or its greater basic character. The fact that at high exchange levels, the amount of NH_3 desorbed is not zero is due to the presence of weak acid sites, primarily of the Lewis type. No physisorbed NH_3 was considered in this experiments or calculations since the samples were flushed in He at 473 K and no appreciable amount of NH_3 was desorbed at low temperatures (Fig. 5).

Therefore, the exchange with Cs and Li allowed us to control the amount of acid sites and the strength of the Lewis acid sites. However the Brönsted acidity seems to remain quite constant for all of the samples studied. It is important to note that some of the exchanged samples present an amount of acid sites similar to that of commercial γ-Al_2O_3 (Table 2).

Conclusions

Several conclusions arise from the studies performed in this work. The XRD and ^{27}Al-MAS-NMR results point out the stability of the zeolite structure during the exchange procedure. The decrease in micropore surface area cannot be explained in terms of an amorphization of the zeolite. This effect needs further study since there was no relation between the size of the cations and the diminution of the surface area. The number and type of acid sites (Brönsted and Lewis) are determined by the amount and type of exchanged cation. ^{133}Cs, ^{6}Li (SUPAS)-MAS-NMR results suggest that cesium cations are located in accessible sites of the zeolite, while Li cations are not.

Acknowledgements

This work was supported by IMP, CoNaCyT (Mexico), and CNRS, SFERE (France) through the PCP Exchange Program No. 33. We acknowledge the important and valuable comments made by the reviewers.

References

1 N. Y. Chen and T. F. Degnan, *Chem. Eng. Prog.*, 1988, **88**, 32.
2 A. Corma, in *Zeolite Microporous Solids: Synthesis, Structure and Reactivity*, eds. E. G. Derouane, F. Lemus, C. Naccache and F. R. Ribeiro, Kluwer Academic Publishers, Dordrecht, The Netherlands, 1992. *Proceedings of the NATO Advanced Study Institute*, Siatra-Estoril, Portugal, May 13–25 1991.
3 A. Corma, *Stud. Surf. Sci. Catal.*, 1989, **49A**, 49.
4 A. W. Chester, R. C. Wilson, S. M. Oleck and J. H. G. Yen, Eur. Pat. 0155822, 1985.
5 N. Y. Chen, W. E. Garwood and F. G. Dwyer, *Shape Selective Catalysis in Industrial Applications*, M. Dekker Inc., New York, 1989, p. 157.
6 D. Barthomeuf, in *Zeolites: Science and Technology*, eds. F. R. Ribeiro, A. E. Rodrígues, L. D. Rollmann and C. Naccache, Martins Nijhoff Publishers, The Netherlands, 1984. *Proceedings of the NATO Advanced Study Institute*, Alcabideche, Portugal, May 1–12, 1983.

7 J. Zheng, J. L. Dong, Q. H. Xu, Y. Liu and A. Z. Yan, *Appl. Catal. A*, 1995, **126**, 141.
8 R. L. Wadlinger, G. T. Kerr and E. J. Rosinski, US Pat. 3,308, 069, 1967.
9 J. Perez–Pariente, J. A. Martens and P. A. Jacobs, *Appl. Catal. A*, 1987, **31**, 35.
10 M. A. Camblor and J. Perez–Pariente, *Zeolites*, 1991, **11**, 202.
11 L. J. Leu, L. Y. Hou, B. C. Kang, C. Li, S. T. Wu and J. C. Wu, *Appl. Catal. A*, 1991, **69**, 49.
12 M. K. Rubin, US Pat. 5,164,169, 1992.
13 M. M. Treacy and J. M. Newsam, *Nature* (*London*), 1988, **332**, 249.
14 S. G. Hedge, R. Kumar, R. N. Bhat and P. Ratnasamy, *Zeolites*, 1989, **9**, 231.
15 P. G. Smirniotis and E. Ruckenstein, *J. Catal.*, 1993, **140**, 526.
16 J. Perez–Pariente, J. Sanz, V. Fornés and A. Corma, *J. Catal.*, 1990, **124**, 217.
17 C. Jia, P. Massiani and D. Barthomeuf, *J. Chem. Soc., Faraday Trans.*, 1993, **89**, 3659.
18 L. Kiricsi, C. Flego, G. Pazzuconi, W. O. Parker Jr., R. Millini, C. Perego and G. Bellusi, *J. Phys. Chem.*, 1994, **98**, 4627.
19 T. Barzetti, Z. Selli, D. Moscotti and L. Forni, *J. Chem. Soc., Faraday Trans.*, 1996, **92**, 1401.
20 T. Bécue, F. J. Maldonado–Hódar, A. P. Antunes, J. M. Silva, M. F. Ribeiro, P. Massiani and M. Kermarec, *J. Catal.*, 1999, **181**, 244.
21 J. Plévert, L. C. de Ménorval, F. Di Renzo and F. Fajula, *J. Phys. Chem. B*, 1998, **102**, 3412.
22 L. C. de Ménorval, J. Plévert, R. Dutartre, F. Di Renzo and F. Fajula, in *Proceedings of the 12th International Zeolite Conference*, ed. M. M. J. Treacy, B. K. Marcus, M. E. Bisher and J. B. Higgens, MRS, Pennsylvania, 1999, Baltimore, Maryland, July 5–10, 1998.
23 F. Rachdi, J. Reichenbach, L. Firlej, P. Bernier, M. Ribet, R. Aznan, G. Zimmer, M. Helmie and M. Mehring, *Solid State Commun.*, 1993, **87**, 547.
24 C. A. Emeis, *J. Catal.*, 1993, **141**, 347.
25 F. J. Maldonado–Hódar, M. F. Ribeiro, J. M. Silva, A. P. Antunes and F. R. Ribeiro, *J. Catal.*, 1998, **178**, 1.
26 F. Fajula, *Stud. Surf. Sci. Catal.*, 1995, **97**, 133.
27 E. Bourget–Lami, P. Massiani, F. Di Renzo, P. Espiau and F. Fajula, *Appl. Catal. A*, 1991, **72**, 139.
28 L. C. de Ménorval, W. Buckermann, F. Figueras and F. Fajula, *J. Phys. Chem.*, 1996, **100**, 465.
29 T. J. Swift, in *NMR of Paramagnetic Molecules*, eds. G. N. La Mar, W. Dew and R. H. Holm, Academic Press, New York, 1973, ch. 2.
30 J. P. Jesson, in *NMR of Paramagnetic Molecules*, eds. G. N. La Mar, W. Dew and R. H. Holm, Academic Press, New York, 1973, ch. 1.
31 C. J. Jameson and J. Masson, in *Multinuclear NMR*, ed. J. Masson, Plenum Press, New York, 1987, ch. 2 and references therein.

Paper a908258a